WM2008 Conference, February 24 -28, 2008, Phoenix, AZ
Abstract #8036

Melted Murataite Ceramics Containing Simulated Actinide/Rare Earth Fraction of High Level Waste

S.V. Stefanovsky, A.G. Ptashkin, O.A. Knyazev, M.S. Zen'kovskaya, O.I. Stefanovsky
State Unitary Enterprise SIA Radon,
7th Rostovskii lane 2/14, Moscow 119121 RUSSIA,

S.V. Yudintsev, B.S. Nikonov, M.I. Lapina
Institute of Geology of Ore Deposits, Petrography, Mineralogy and Geochemistry of the Russian Academy of Sciences (IGEM RAS)
Staromonetny lane 35, Moscow 119017 RUSSIA

ABSTRACT

Murataite-based ceramics with three different chemical compositions containing simulated actinide/rare earth (RE) fraction of HLW were produced in a resistive furnace at a temperature of 1500 °C and two of them – in a cold crucible energized from a 5.28 MHz/10 kW high frequency generator. All the samples prepared in resistive furnace were composed of major murataite and minor perovskite, crichtonite, zirconolite, and pyrophanite/ilmenite. The samples produced in the cold crucible were composed of murataite, perovskite, crichtonite, and rutile. Higher content of perovskite and crichtonite in the cold crucible melted ceramic than in the ceramic with the same chemical composition but melted in resistive furnace may be due to higher temperature in the cold crucible (up to 1600-1650 °C) at which some fraction of murataite was subjected to decomposition yielding additional amount of perovskite and crichtonite. Method of melting may effect on elemental partitioning in the murataite-containing ceramics because light (Ce-group) REs enter preferably perovskite phase whereas Nd, Sm, and heavy (Y-group) REs are accommodated in the murataite polytypes. Thus, perovskite and murataite are major host phases for the Ce- and Y-group REs, respectively, whereas tetravalent actinides (U) enter muratatite only.

INTRODUCTION

Murataite-containing ceramics are considered to be promising actinide/rare earth (An/RE) waste forms [1]. They may be produced by both ceramic (cold pressing and sintering) and melting routes. An important feature of murataite melts is gradual segregation of the murataite polytypes yielding zoned grains with the highest An/RE content in their core and the lowest – in the rim and thus suppressing leaching of these elements. The melting temperature has been shown to be ranged between ~1400 °C and ~1600 °C depending on chemical composition. One of the most effective melting technologies to be potentially applied for murataite ceramic production is an inductive cold crucible melting (ICCM) [2,3]. This process is high productive due to active hydrodynamic regime and the cold crucible melter is small-sized and has no refractories and electrodes contacting with melt that provides for its long lifetime.

Successful demonstration of ICCM production of the U- and Th-bearing murataite ceramics [2,3] allows transfer to the next step – production of murataite ceramics containing a surrogate of

An/RE fraction of high level waste (HLW). The An/RE fraction contains major La and some Ce-group lanthanides (Ce, Pr, Nd, Sm, traces of Pm, Eu and Gd) and minor Np, Am and Cm as well as residual U and Pu. Zr may be also present. Partitioning of these elements among co-existing phases, especially murataite and perovskite, in the murataite ceramics may effect on phase composition, leachability and radiation resistance of the ceramic waste form.

The goal of this work is comparative study of phase composition and elemental partitioning among co-existing phases in the murataite-containing ceramics produced in lab-scale crucibles in a resistive furnace and cold crucible.

EXPERIMENTAL

Baseline chemical composition of the murataite ceramic is (wt.%): 5.0 Al_2O_3, 10.0 CaO, 55.0 TiO_2, 10.0 MnO, 5.0 Fe_2O_3, 5.0 ZrO_2, 10 WO (WO = waste oxides) [4]. In total 10 wt.% An/RE oxides were introduced and target chemical compositions of the ceramics are given in Table I.

Table I. Chemical compositions (wt.%) of the An/RE-bearing ceramics.

Oxides	1	2	3	4
Al_2O_3	5.0	5.0	5.0	4.0
CaO	10.0	10.0	10.0	8.0
TiO_2	55.0	55.0	55.0	59.0
MnO	10.0	10.0	10.0	8.0
Fe_2O_3	5.0	5.0	5.0	4.0
ZrO_2	5.0	4.0	3.0	8.2
La_2O_3	1.25	1.25	1.25	1.0
Ce_2O_3	2.48	2.48	2.48	1.98
Pr_6O_{11}	1.23	1.23	1.23	0.98
Nd_2O_3	3.96	3.96	3.96	3.17
Sm_2O_3	0.73	0.73	0.73	0.59
Eu_2O_3	0.20	0.20	0.20	0.16
Gd_2O_3	0.15	0.15	0.15	0.12
UO_2	-	1.0	2.0	0.8

The ceramic batches for lab-scale tests were prepared from reagent-grade oxides intermixed and mechanically-activated in an AGO-2U planetary mill for 5 min under an acceleration of 50g. The mixtures were placed in 50 mL glassy carbon crucibles, heated to a temperature of 1500 °C at a rate of 5 °C/min, kept at this temperature for 0.5 hr and then the melts were crystallized by controlled cooling to 1300 °C at a rate of ~2 °C/min followed by spontaneous cooling to room temperature in turned-off furnace.

The ceramic batches for the cold crucible tests were prepared in amount of 1 kg from the same oxides intermixed in a ball-mill. The ceramics were produced in a small-scale unit with a 56 mm inner diameter copper cold crucible energized from a 5.28 MHz/10 kW generator (Figure 1).

The samples were examined with X-ray diffraction using a DRON-4 diffractometer (Fe K-radiation, voltage is 40 KeV, beam current is 30 mA, dwell time is 0.6 s, step size is 0.05 deg., 2-

theta ranged between 10 and 90 deg., and Si as an internal standard) and scanning electron microscopy with energy dispersive system (SEM/EDS) using a JSM 5610 LV + JED-2300 unit (voltage is 25 KeV, beam current is 1 nA, probe diameter is 1 to 3 μm, dwell time is 100 s; metals, oxides and fluorides were used as standards).

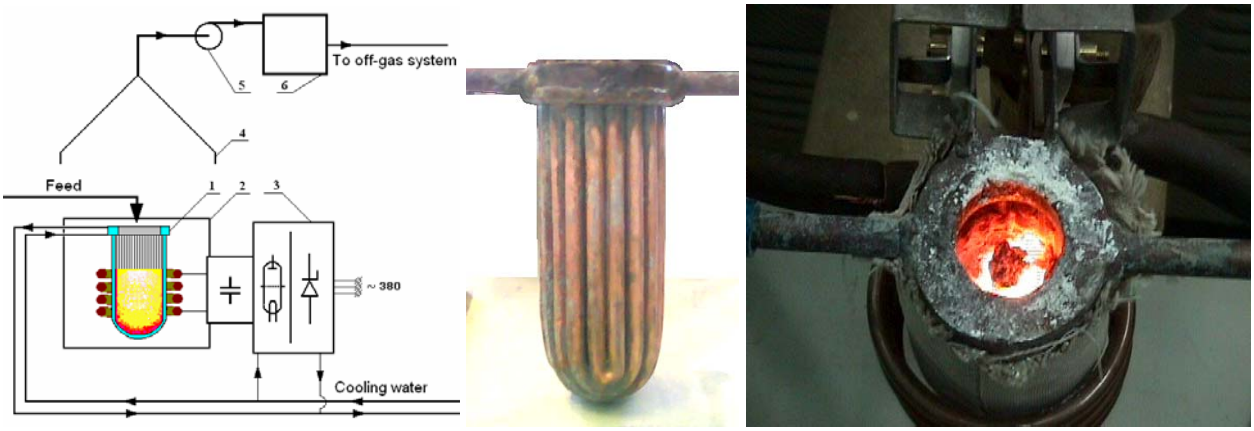

Figure 1. Flowsheet of the small-scale cold crucible unit (left), view of the copper cold crucible (middle) and view of cold crucible with murataite melt (right).
1 – cold crucible with inductor, 2 – process box, 3 – high-frequency generator, 4 – off-gas umbrella and pipe, 5 – fan, 6 – HEPA filter.

To start-up the ICCM process a portion of the batch was fed into the cold crucible and a graphite rod was inserted within to provide for initial batch heating and to create a starting melt followed by increase of input power to enlarge starting melt volume. Upon achieving the steady-state conditions the batch was fed into the cold crucible in 50-80 g portions, with keeping until their complete melting before feeding of the next portion. In the test on production of the ceramic 2c with composition No.2 (Table I) average melting rate, specific melt rate (productivity), and melting ratio were 0.8 kg/hr, ~330 kg/(m^2×hr), and ~7.6 kW×h/kg. At the production of the ceramic 4c with composition No.4 these parameters were as follows: 0.7 kg/hr, ~285 kg/(m^2×hr), and ~7.5 kW×h/kg. Open melt temperature measured by optical pyrometer ranged between 1380 and 1550 °C. Melting of the composition 2c was performed at a temperature closer to upper limit of this range. The second composition has some lower melting temperature – up to 1450-1500 °C. Better melting conditions of the ceramic 4c may be due to higher electric conductivity of the melt with higher TiO_2 content.

RESULTS

As follows from XRD patterns of the samples produced in glassy carbon crucibles (Figure 2) all the ceramics were composed of major murataite polytypes (55-65 % of total), secondary in abundance perovskite and crichtonite (15-20 % each) and minor pyrophanite/ilmenite (10-15 % of total). UO_2 substitution for ZrO_2 results in minor changes in phase composition of the ceramics.

The major peak within the range of 2.86…2.80 Å is a superposition of the peaks due to three different murataite polytypes (Figure 2, detail) with five- (M5, d =2.84-2.85 Å), eight- (M8, d=2.82-2.83 Å) and three-fold (M3, d=2.80-2.81 Å) elementary fluorite unit cell. One of the crichtonite reflections is overlapped with the murataite reflections as well.

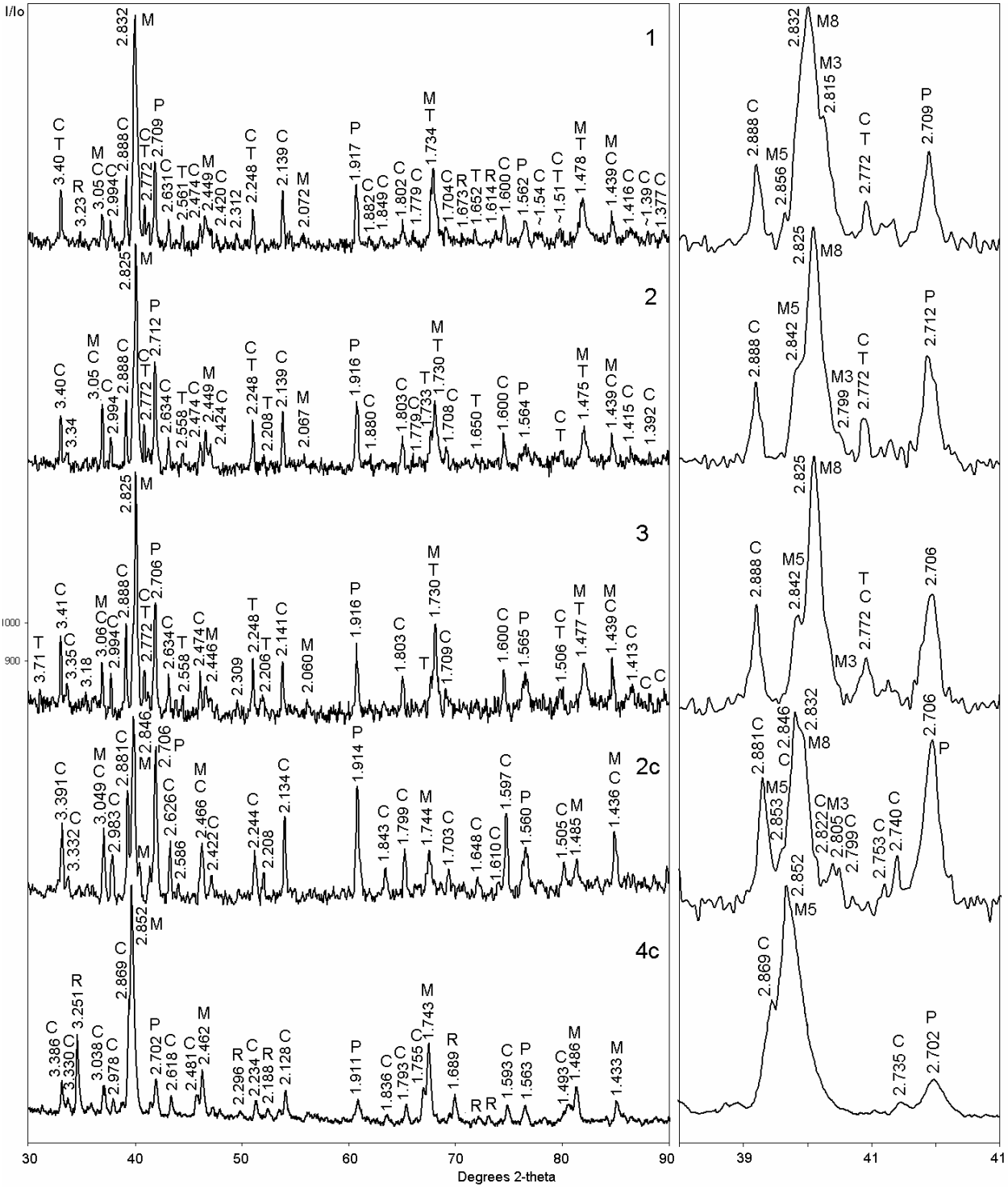

Figure 2. XRD patterns of the ceramics produced in glassy carbon crucibles in laboratory furnace (1, 2, and 3) and in cold crucible (2c and 4c) and fragments within the angular range of the strongest reflection.

C – crichtonite, M – murataite (M5, M8, M3 – polytypes with five-, eight-, and three-fold fluorite unit cell), P – perovskite, R – rutile, T – pyrophanite/ilmenite.

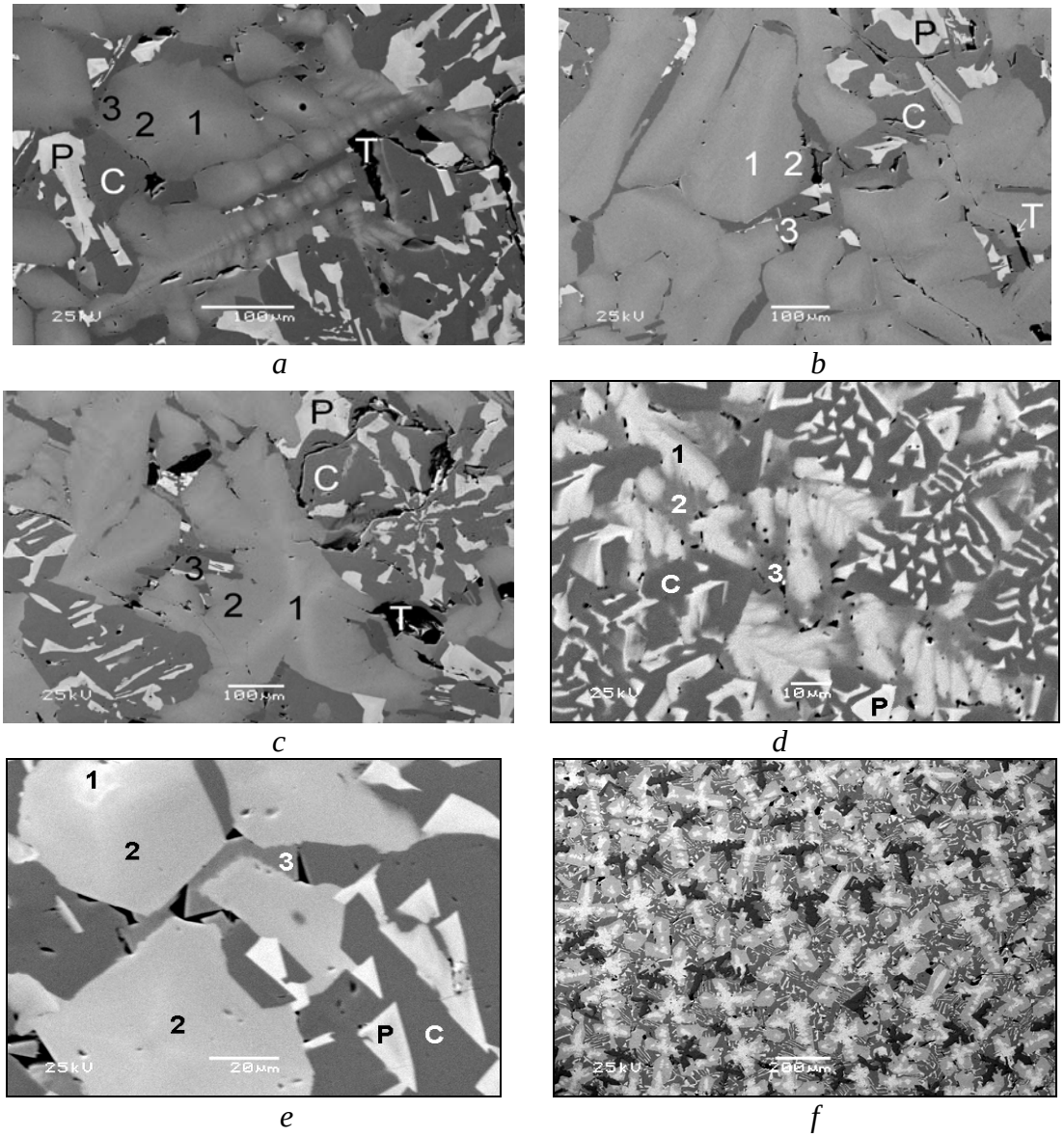

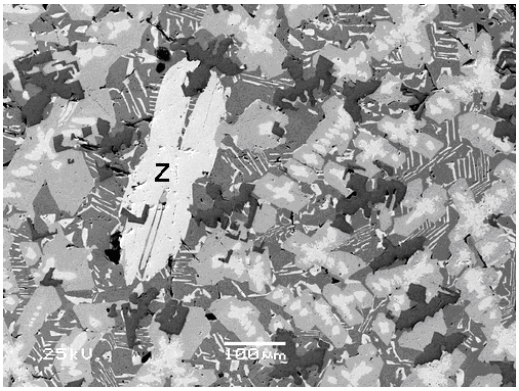

g

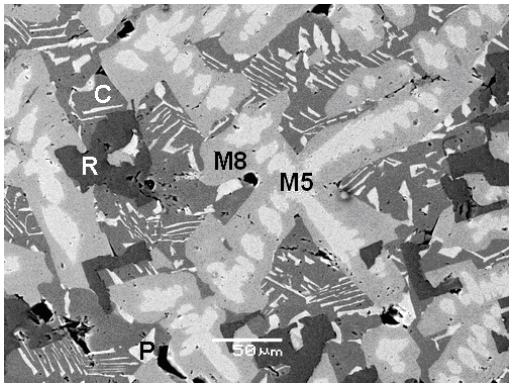

h

Figure 3. SEM images of the ceramics 1 (*a*), 2 (*b*), 3 (*c*), 2c (*d, e*), and 4c (*f*-*h*).

(*e*) is detail of (*d*) and (*g*), (*h*) are details of (*f*). 1,2,3 – M5, M8, M3; C – crichtonite, P – perovskite, R – rutile, T – pyrophanite/ilmenite, Z – zirconolite.

Table II. Chemical compositions (wt.%) of co-existing phases in the ceramics produced in glassy carbon crucibles in resistive furnace.

Oxides	1						2						3					
	M5	M8	M3	C	T	P	M5	M8	M3	C	T	P	M5	M8	M3	C	T	P
Al_2O_3	3.85	5.03	8.9	4.66	*0.43*	1.04	4.54	6.87	10.49	4.93	*0.46*	1.08	5.18	6.45	9.6	4.95	0.47	1.38
CaO	5.92	6.84	6.73	3.33	*0.37*	20.09	7.36	6.27	6.54	2.75	*0.59*	21.42	5.55	6.1	6.04	3.23	0.77	21.21
TiO_2	48.54	53.03	52.45	67.56	54.23	47.95	53.4	52.68	52.34	65.95	53.53	49.15	49.02	48.74	47.93	68.12	53.42	48.18
MnO	12.95	12.35	11.54	8.52	27.82	1.56	11.35	13.19	12.31	8.84	28.71	2.4	14.34	12.92	12.48	8.48	29.11	2.48
Fe_2O_3	4.44	5.71	8.85	4.59	19.52	nd	4.61	7.37	9.02	5.45	19.74	nd	6.46	7.31	8.57	5.62	18.34	0.91
ZrO_2	15.5	9.5	4.22	4.28	nd	nd	7.65	4.64	2.55	3.21	nd	nd	9.65	7.03	3.76	2.65	nd	nd
La_2O_3	*0.82*	*0.6*	1.07	1.42	nd	2.34	1.26	*0.87*	*0.55*	*0.99*	nd	2.15	*0.45*	*0.45*	*0.7*	*0.94*	nd	2.57
Ce_2O_3	1.43	1.55	2.01	2.02	nd	7.46	2.28	2.09	1.97	2.13	nd	7.62	1.24	1.89	2.34	2.25	nd	6.71
Pr_2O_3	*0.75*	1.09	*0.63*	nd	nd	3.44	*0.74*	*0.76*	*0.92*	1.29	nd	3.96	*0.84*	*0.49*	*0.81*	1.15	nd	3.34
Nd_2O_3	2.4	2.67	2.67	1.17	nd	10.6	3.68	2.69	2.18	2.15	nd	9.56	1.62	1.87	2.81	1.52	nd	10.24
Sm_2O_3	*0.75*	1.03	*0.34*	*0.81*	nd	2.3	*0.37*	nd	*0.24*	*0.47*	nd	1.72	*0.63*	*0.55*	*0.38*	*0.63*	nd	1.61
Eu_2O_3	*0.44*	nd	*0.47*	nd	nd	1.03	nd	nd	*0.44*	*0.37*	nd	nd	*0.48*	*0.65*	nd	nd	nd	*0.33*
Gd_2O_3	*0.52*	nd	nd	nd	nd	*0.6*	nd	nd	*0.23*	nd	nd	*0.68*	nd	nd	nd	nd	nd	nd
UO_2	-	-	-	-	-	-	2.18	0.93	*0.61*	*0.86*	nd	nd	5.36	4.13	2.35	1.07	nd	1.24
Total	98.31	99.4	99.88	98.36	102.37	98.41	99.42	98.36	100.39	99.39	103.03	99.74	100.82	98.58	97.77	100.61	102.11	100.20

nd – not detected (below detection limit), italics – values <2 sigma.

SEM images (Figure 3) show that the murataite forms large (up to 100-150 μm in size) zoned grains whose core (the lightest), intermediate zone, and rim (the darkest) are composed of the M5, M8, and M3 polytypes, respectively. Light- and dark-gray grains are perovskite and crichtonite and the darkest inclusions are pyrophanite/ilmenite. Chemical compositions of the phases are given in Table II.

Murataite polytypes are major hosts for Zr and U. Their contents are reduced from the M5 to M3 polytype. La and Ce-group lanthanides are partitioned among murataite, perovskite and crichtonite. At that, La, Ce, Pr and Nd are preferably concentrated in perovskite, whereas Eu and Gd are equally partitioned between perovskite and murataite. Crichtonite also accumulates rare earths. It is surprise appreciable Eu concentration in pyrophanite/ilmenite. Probably some fraction of Eu exists in a divalent form substituting for Fe^{2+} and Mn^{2+} ions in their sites in the structure of Fe/Mn-titanate. In the U-bearing samples (2 and 3) minor U enters crichtonite. In the sample No.2 two perovskite varieties with some different chemical compositions have been found. One of them (P-1) is enriched with Nd and Sm and contains U and the second one (P-2) is enriched with La, Ce and Gd.

The ceramic with chemical composition No.2 produced in the cold crucible (Sample 2c) is composed of the same phases as Sample 2 produced in glassy carbon crucible (Figures 2 and 3). The schematic view of the cold crucible with solidified ceramic block and view of ceramic pieces are shown on Figure 4. Upper part of this block is dense ceramic composed of grains whose size increases from rim towards core of the block. Zone of the porous material with significant amount of gas bubbles is located below. The zone located near the crucible bottom is composed of unmelted or partially-melted batch. The melt was very “short” and thickness of the “skull” does not exceed 1 mm.

The sample 2c has dark-gray color and massive texture. It is composed of major murataite and perovskite and minor crichtonite. Because ceramic block is not uniform on both texture and phase composition, perovskite dominates over murataite in the rim and in the near surface area whereas in the core the murataite is predominant. Three murataite polytypes: M5, M8 and M3 were found. Perovskite and crichtonite form aggregates because they were segregated simultaneously from an eutectic melt. Murataite in the rim forms grains with poorly appeared zoning which are located among the perovskite/crichtonite aggregate. In the center of the block, where perovskite and crichtonite content is lower, murataite forms regular zoned grains whose core and rim are composed of the M5 and M8 polytypes, respectively. The M3 polytype exists as individual grains overgrown the crystals of the M8 polytype (Figure 3, *e*).

Murataite polytypes are major hosts for U (Table III). Its concentrations in perovskite and crichtonite are lower than the detection limit (0.2 wt.%). Like in all other matrices, U content is reduced from M5 (4.6 wt.%) to M3 (2.3 wt.%). Rare earths enter murataite, perovskite and crichtonite being variously partitioned among them depended on elemental ionic radii. Larger-sized Ce-group elements (from La to Nd) are markedly partitioned in the favor of perovskite but reduction of ionic radius makes elemental partitioning more uniform. These are represented by reduction of distribution factor of rare earths – $K_{P/M5}$ between perovskite (P) and the M5 polytype from 5 (for La, Pr and Nd) to 2 and lower (for Sm, Eu and Gd). Total RE content in the M5 and M8 polytypes is 7.4 wt.%, in the M3 polytype and crichtonite this value is 5.0 wt.%. The highest RE concentration (24.9 wt.%) was found to be in perovskite. The latter effects substantially on immobilization properties of the matrices with respect to actinides. Perovskite is

known to have the lowest durability in solutions because it has the highest ratio of large low-charged (Ca^{2+}) to small high-charged (Ti^{4+}) cations. Because elemental release rate from perovskite is the highest its occurrence in ceramics is believed to be a negative factor.

Total content of tetravalent actinides (U^{4+}, Th^{4+}, Np^{4+}, Pu^{4+}) is low, normally, lower than the detection limit (Table III). Trivalent actinides (Am^{3+}, Cm^{3+}, Pu^{3+}) are expected to have higher content in perovskite as it follows from high content of Ce-group REs having similar ionic radii.

Table III. Chemical compositions (wt.%) of the phases in the ICCM ceramics by SEM/EDS data.

Oxides	2c					4c					
	M5	M8	M3	C	P	Z	M5	M8	C	P	R
Al_2O_3	2.88	3.97	9.69	6.60	1.21	1.79	1.93	3.77	5.98	1.60	0.79
CaO	8.04	9.37	7.83	3.90	23.27	9.31	8.75	9.25	4.03	19.69	0.73
TiO_2	47.32	51.63	49.49	62.72	48.48	48.20	47.86	53.34	64.60	50.25	88.82
MnO	12.20	10.80	15.42	10.80	1.28	4.26	7.54	8.88	10.38	2.03	0.56
Fe_2O_3	3.66	4.13	6.12	7.19	0.84	2.25	2.72	4.08	6.66	1.30	0.71
ZrO_2	14.19	8.99	4.42	3.06	nd	21.15	20.72	9.59	2.54	nd	8.65
La_2O_3	*0.47*	nd	nd	1.22	2.31	0.15	0.25	0.58	1.11	3.28	nd
Ce_2O_3	2.60	2.68	1.79	1.60	5.67	2.10	2.07	2.63	1.61	6.36	nd
Pr_2O_3	*0.71*	*0.66*	*0.71*	*0.47*	3.6	1.01	*0.56*	*0.84*	*0.72*	3.36	nd
Nd_2O_3	2.34	2.97	1.78	1.70	11.09	4.48	3.82	3.11	1.48	9.15	nd
Sm_2O_3	*0.69*	*0.68*	*0.48*	nd	1.45	0.93	0.91	*0.32*	nd	1.11	nd
Eu_2O_3	*0.27*	*0.41*	*0.46*	nd	*0.38*	*0.38*	*0.50*	*0.21*	nd	nd	nd
Gd_2O_3	*0.33*	nd	nd	nd	*0.42*	*0.36*	*0.60*	nd	nd	nd	nd
UO_2	4.55	3.06	2.27	nd	nd	1.77	1.81	1.44	nd	nd	nd
Total	100.25	99.35	100.46	99.26	100.00	98.14	100.04	98.04	99.11	98.13	100.26
Σ РЗЭ	7.41	7.40	5.22	4.99	24.92	9.41	8.72	7.69	4.92	23.26	nd
Ions	Number of atoms in the calculated chemical formulae										
Al^{3+}	0.71	1.65	1.59	2.10	0.04	0.12	0.48	0.90	1.90	0.05	0.01
Ca^{2+}	1.81	3.55	1.16	1.13	0.65	0.59	2.03	5.00	1.16	0.55	0.01
Ti^{4+}	7.49	13.73	5.17	12.75	0.95	2.15	7.76	13.47	13.10	0.98	0.92
Mn^{2+}	2.17	3.23	1.81	2.47	0.03	0.21	1.37	3.79	2.37	0.04	0.01
Fe^{3+}	0.58	1.10	0.64	1.46	0.02	0.10	0.44	0.62	1.35	0.03	0.01
Zr^{+4}	1.46	1.55	0.30	0.40	-	0.61	2.18	1.57	0.33	-	0.06
La^{3+}	0.04	-	-	0.12	0.02	0.00	0.04	0.04	0.11	0.03	-
Ce^{3+}	0.20	0.35	0.09	0.16	0.05	0.05	0.15	0.19	0.16	0.06	-
Pr^{3+}	0.05	0.09	0.04	0.05	0.03	0.02	0.04	0.06	0.07	0.03	-
Nd^{3+}	0.18	0.38	0.09	0.16	0.10	0.09	0.30	0.22	0.14	0.09	-
Sm^{3+}	0.05	0.08	0.02	-	0.01	0.02	0.07	0.02	-	0.01	-
Eu^{3+}	0.02	0.05	0.02	-	0.00	0.01	0.04	0.01	-	-	-
Gd^{3+}	0.02	-	-	-	0.00	0.01	0.04	0.00	-	-	-
U^{4+}	0.21	0.24	0.07	-	-	0.02	0.07	0.11	-	-	-
ΣCat.	15.00	26.00	11.00	20.82	1.91	4.01	15.00	26.00	20.70	1.87	1.01
ΣO^{2-}	27-x	47-x	20-x	36.00	3.00	7.00	27-x	47-x	36.00	3.00	2.00

nd – not detected (below detection limit), italics – values <2 sigma.

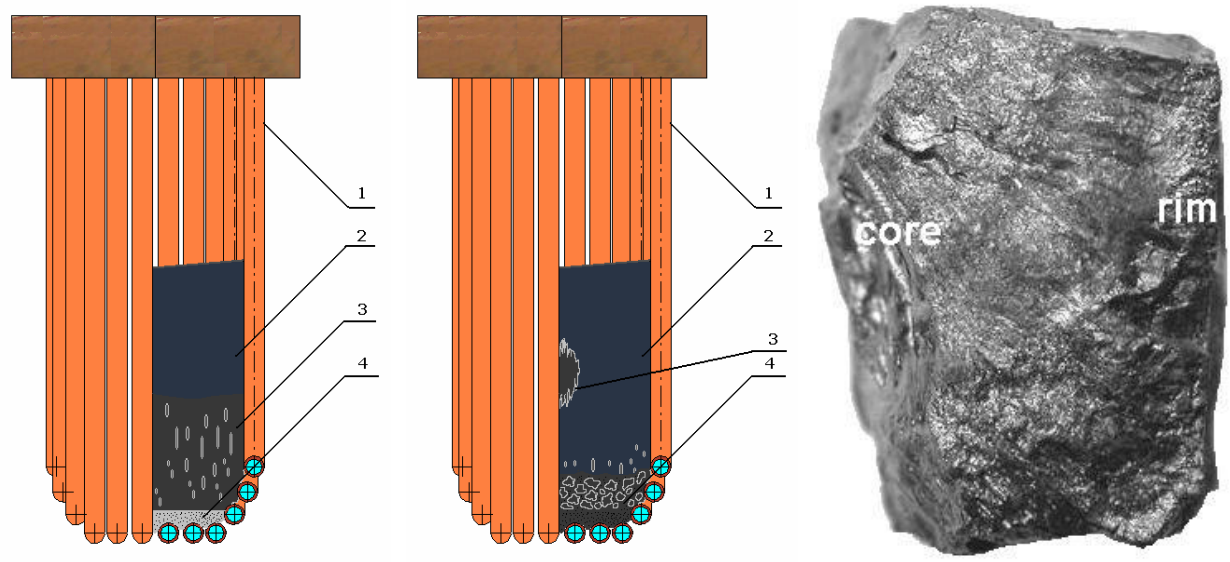

Figure 4. Schematic view of the cold crucible with ceramic 2c (left), 4c (middle) and view of fragment of the 2c ceramic (right).
Left: 1 – cold crucible wall, 2 – dense ceramic, 3 – porous ceramic, 4 – unmelted batch; Middle: 1 – cold crucible walls, 2 – dense ceramic, 3 – shrink hole, 4 – unmelted batch.

Thus, the composition No.2 in Table I cannot be considered as suitable matrix for the immobilization of the An/RE fraction of HLW due to occurrence of major perovskite that may cause worsening of immobilization properties of the matrix due to increase of actinides and rare earths release into environment. Therefore, the composition No.2 has been modified by addition of TiO_2 and ZrO_2 (3:1) in amount of 20 wt.% to achieve a composition No.4 (Table I).

The ceramic with the composition No.4 (Sample 4c) produced by ICCM and crystallization has a shrink hole but the rest of the block is composed of dense ceramic with uniform massive texture consisting of murataite (55-60 vol.%), crichtonite (15-20 vol.%) , perovskite (10-15 vol.%), rutile (10-15 vol.%), and zirconolite (≤5 vol.%) - Figures 2 and 3. Occurrence of zirconolite and rutile differ the present ceramic from the previous sample (2c). The other difference is much higher murataite and lower perovskite content. Thus, the phase composition of the ceramic was optimized in the favor of increase of the content of the target phases being high chemical resistant hosts for actinide elements.

Murataite forms zoned grains typical of segregation from the melt and composed of the M5 polytype in the core and the M8 polytype in the rim (Figure 3, *h*). Perovskite and crichtonite are observed as aggregates segregated simultaneously from the eutectic melt. Rutile looks like skeleton-type crystals. Zirconolite forms individual elongated crystals (Figure 3, *g*).

Chemical compositions of co-existing phases are given in Table III. The highest Zr content is a characteristic of the zirconolite. The M5 polytype also has high Zr content comparable to the zirconolite phase. Zr content in the M8 polytype is by ~2 times lower. Minor Zr enters crichtonite (~2.5 wt.%). It should be noted quite high ZrO_2 content in rutile (8.7 wt.%) that is rather typical of high-temperature processes where isomorphic substitution $Zr^{4+} \Leftrightarrow Ti^{4+}$ in the

rutile lattice is facilitated. Total REs content is the highest in the perovskite phase, some lower in zirconolite and murataite and the lowest in the crichtonite. However, due to much higher murataite content in the ceramic major REs fraction is accumulated by this phase. Uranium is partitioned between murataite and zirconolite but, taking into account that murataite content is much higher than zirconolite, murataite (both M5 and M8 polytypes) is major host phase for U in this ceramic.

DISCUSSION

Figures 2 and 3 demonstrate similar phase composition of the ceramics Nos. 1-3 prepared in a resistive furnace. They are composed of major murataite (three polytypes: M5, M8, and M3), secondary in abundance crichtonite and perovskite and minor Fe/Mn-titanate (pyrophanite/ ilmenite). In particular, the ceramic with target chemical composition No.2 (Table I) contains ~50-55 vol.% murataite, ~20-25 vol.% crichtonite, ~20-25 vol.% perovskite, and ~5 vol.% Fe/Mn titanate. The major bulk of this sample is formed by zoned murataite grains composed of the M5 polytype in the core, the M8 polytype in the intermediate zone and the M3 in the rim. The interstitials between them are filled with the crichtonite/perovskite aggregates. The murataite is major host for uranium. REs are partitioned among all the phases and their distribution depends on atomic number (ionic radius) of the element (Tables II and III). The light REs (La…Sm, and Gd) enter preferably perovskite; Eu is concentrated in the murataite polytypes. Some REs fraction enters crichtonite.

The sample 2c with the same composition No.2 but produced in the cold crucible has lower murataite (~35-40 vol.%) and higher perovskite (~30-35 vol.%) and crichtonite (~25-30 vol.%) contents. Chemical compositions (Table III) of the murataite polytypes may be recalculated (taking into account occurrence of Mn^{3+} [5] and distribution of Fe^{3+} ions over six- and five-coordinated sites in a ratio of 3:1 [6]) to crystal chemical formulae $(Ca_{1.81}Mn^{2+}_{0.96}Zr_{1.46}La_{0.04}Ce_{0.20}Pr_{0.05}Nd_{0.18}Sm_{0.05}Eu_{0.02}Gd_{0.02}U_{0.21})^{VIII}(Ti_{6.85}Fe_{0.44}Al_{0.71})^{VI}(Mn^{3+}_{1.21}Fe_{0.15}Ti^{4+}_{0.64})^{V}O_{25.70}$ (M5), $(Ca_{3.55}Mn^{2+}_{1.71}Zr_{1.55}Ce_{0.35}Pr_{0.09}Nd_{0.38}Sm_{0.08}Eu_{0.05}U_{0.24})^{VIII}(Ti_{11.53}Fe_{0.82}Al_{1.65})^{VI}(Mn^{3+}_{1.52}Fe^{3+}_{0.28}Ti_{2.20})^{V}O_{44.13}$ (M8), and $(Ca_{1.16}Mn^{2+}_{1.21}Zr_{0.30}Ce_{0.09}Pr_{0.04}Nd_{0.09}Sm_{0.02}Eu_{0.02}U_{0.07})^{VIII}(Ti_{3.93}Fe_{0.48}Al_{1.59})^{VI}(Mn^{3+}_{0.60}Fe^{3+}_{0.16}Ti_{1.24})^{V}O_{18.09}$ (M3). U enters predominantly murataite, whereas major REs are concentrated in perovskite. Minor REs enter crichtonite. Trivalent actinides are expected to exhibit the same behavior. High perovskite content in the ceramics may worsen their chemical durability due to elevated REs release from higher soluble perovskite phase.

Thus, the major difference between the ceramics prepared in small glassy carbon and larger size cold crucible is higher content of additional phases – perovskite and crichtonite in the latter. The possible reason of this is a high-temperature decomposition of the murataite phases yielding extra perovskite and crichtonite with corresponding re-distribution of waste elements between the phases.

Modification of the ceramic composition in the favor of preferable murataite formation (modified composition also has lower melting temperature) reduces amount of extra phases (25-35 vol.% of total) but yields zirconolite which, however, offers minor effect on elemental partitioning because of its low content in the ceramic (≤5 vol.%).

Murataite (55-65 vol.% of total) remains major host phase for U and REs. Crystal chemical formulae of the M5 and M8 polytypes recalculated from analytical data (Table III) are as

follows: $(Ca_{2.03}Mn^{2+}_{0.04}Zr_{2.18}La_{0.04}Ce_{0.15}Pr_{0.04}Nd_{0.30}Sm_{0.07}Eu_{0.04}Gd_{0.04}U_{0.07})^{VIII}(Ti_{7.19}Fe_{0.33}Al_{0.48})^{VI}(Mn^{3+}_{1.33}Fe_{0.11}Ti^{4+}_{0.56})^{V}O_{26.47}$ and $(Ca_{5.00}Mn^{2+}_{0.78}Zr_{1.57}La_{0.04}Ce_{0.19}Pr_{0.06}Nd_{0.22}Sm_{0.02}Eu_{0.01}U_{0.11})^{VIII}(Ti_{12.64}Fe_{0.46}Al_{0.90})^{VI}(Mn^{3+}_{3.01}Fe^{3+}_{0.16}Ti_{0.83})^{V}O_{43.69}$. Like in the ceramics containing 10 wt.% RE_2O_3 (RE = Ln, Ce, Pr) light REs form the perovskite-type phase whereas Zr^{4+} ions substitute for them in the eight-coordinated sites in the structure of the murataite polytypes [7]. This explains anomalously high ZrO_2 content in the murataite phase, especially the M5 polytype (Table III). Excess of Zr favors formation of the zirconolite phase.

CONCLUSION

Ceramics for immobilization of the An/RE fraction of HLW prepared in both small glassy carbon crucibles in resistive furnace and in larger-sized cold crucible are composed of the same major phases – murataite, perovskite and crichtonite. The ceramic based on baseline murataite composition produced in the cold crucible has higher content of perovskite and crichtonite than the ceramic prepared in resistive furnace. Because REs are partitioned in the favor of perovskite, the baseline composition was modified towards increasing of TiO_2 and ZrO_2 concentrations to reduce content of the extra phases. As a result murataite content in the ceramic was increased to 55-65 vol.% of total bulk of the ceramic and it is major host phase for uranium and rare earths.

ACKNOWLEDGEMENTS

The work was performed under financial support from the Russian Federal Agency on Science and Innovations (State Contract No. 02.516.11.6048) and Russian Foundation for Basic Research (grant # 07-05-13502-ofi).

REFERENCES

1. S.V. STEFANOVSKY, S.V. YUDINTSEV, B.S. NIKONOV, B.I. OMELIANENKO, and A.G. PTASHKIN, **"**Murataite-Based Ceramics for Actinide Waste Immobilization," Mat. Res. Soc. Symp. Proc. 556 (1999) 121-128.
2. S.V. STEFANOVSKY, O.I. KIRJANOVA, S.V. YUDINTSEV, and O.A. KNYAZEV, "Cold Crucible Melting of Murataite-Containing Ceramics," Proc. Waste Management '01. Conf. Tucson, AZ. February 25 – March 1, 2001. CD-ROM. ID 324.
3. S.V. STEFANOVSKY, A.G. PTASHKIN, O.A. KNYAZEV, S.A. DMITRIEV, S.V. YUDINTSEV, and B.S. NIKONOV, "Inductive Cold Crucible Melting of Actinide-Bearing Murataite-Based Ceramics," Journ. Alloys Compd. 444-445 (2007) 438-442.
4. S.V. YUDINTSEV, S.V. STEFANOVSKY, B.S. NIKONOV, and B.I. OMELIANENKO, "Phase and Chemical Stability of Murataite Containing Uranium, Plutonium and Rare Earths," Mat. Res. Soc. Symp. Proc. 663 (2001) 357-366.
5. S.V. STEFANOVSKY, S.V. YUDINTSEV, B.S. NIKONOV, and A.A. SHIRYAEV, "Valence State of Iron, Manganese and Gadolinium in Murataite Ceramic for Immobilization of REEs and Actinides," The Fifth Russian Conference on Radiochemistry "Radiochemistry-2006". Abstracts. Dubna, Russia, October 23-27, 2006, pp. 212-213 (2006).
6. V.S. URUSOV, V.S. RUSAKOV, S.V. YUDINTSEV, and S.V. STEFANOVSKY, "Examination of Synthetic Murataite Structure Using Data of Mössbauer Spectroscopy," Mat. Res. Soc. Symp. Proc. 807 (2004) 243-248.

7. S. STEFANOVSKY, S. YUDINTSEV, B. NIKONOV, and O. STEFANOVSKY, “Rare Earth Bearing Murataite Ceramics,” Mat. Res. Soc. Symp. Proc. 985 (2007) 0985-NN04-10.